Armenian Journal of Physics, 2022, vol. 15, issue 4, pp. 175-181

Polaronic Effects on the Electron Raman Scattering in a Spherical Anisotropic Quantum Dot

T.K. Ghukasyan[1*], A.L. Asatryan[1], L.A. Vardanyan[2],
A.A. Kirakosyan[1], A.L. Vartanian[1]

[1]*Department of Solid State Physics, Yerevan State University, 1, Al. Manoogian, Yerevan 0025, Armenia*
[2]*Center of Sciences and Advanced Technologies, Norashen 45-99, Yerevan, 0048, Armenia*

*Email: tigran.ghukasyan@ysu.am

(Received: November 5, 2022; Revised: December 5, 2022; Accepted: December 8, 2022)

Abstract. We study the polaronic effect on the differential cross section (DCS) for an electron Raman scattering process in a spherical anisotropic semiconductor quantum dot in the presence of a homogeneous external electric field. The Fröhlich coupling of electrons with confined and surface polar optical phonon modes for resonance Raman scattering is considered. The influence of electron-phonon coupling on the energy spectrum is taken into account in the framework of perturbation theory. The emission spectra are discussed for different anisotropy cases. Resonant peaks in the spectra are found and interpreted.

Keywords: Raman scattering, polaronic effect, quantum dot

DOI: 10.54503/18291171-2022.15.4-175

1. Introduction

Semiconductor quantum dots (QDs) are widely used in modern electronics and quantum technologies not only due to the availability of fabrication and the ability to connect to solid state systems [1], but also due to the design capabilities of their electronic and phonon spectra, which are determined by structural parameters (size, shape). Therefore, the study of the electronic and phonon spectra of QDs provides valuable information about their material composition and structural parameters, such as the size and shape of QDs, as well as mechanical deformations and mixing of atoms in the system. Features of the interaction of light and quantum dots, the probability of which depends significantly both on the energy spectrum of charge carriers and on the features of the phonon system, is manifested when Raman scattering processes are considered. Therefore, among optical methods, Raman spectroscopy is the most informative method for determining the quasiparticle spectra of semiconductor nanostructures. Experimental research on Raman scattering in nanocrystals has been extensively reported [2-7]. To interpret experimental results, theoretical research usually focus on the calculation of the differential cross section for Raman scattering [8-11].

In this work, we consider Raman scattering of light in a quantum dot of spherical symmetry in a nonpolar dielectric matrix. It is assumed that, in comparison with electrons, the contribution of holes to the Raman scattering intensity can be neglected. The electron-phonon interaction of the Frohlich type is considered within the framework of the dielectric continuum model. Stokes processes were studied in the scattering of electrons both by bulk and surface phonons.

2. Theory

2.1 Electronic states in a spherical quantum dot

We consider a spherical quantum dot (QD) with an anisotropic parabolic confining potential in an external uniform electric field $\boldsymbol{F}$. Choosing the z axis along the electric field, the Hamiltonian of the system in the effective mass approximation can be written as

$$\widehat{H}_0 = \frac{\hat{p}_x^2}{2m^*} + \frac{1}{2}m^*\omega_{0x}^2 x^2 + \frac{\hat{p}_y^2}{2m^*} + \frac{1}{2}m^*\omega_{0y}^2 y^2 + \frac{\hat{p}_z^2}{2m^*} + \frac{1}{2}m^*\omega_{0z}^2 z^2 + |e|Fz, \tag{1}$$

where m^* is the electron effective mass, e is the electron charge, ω_{0x}, ω_{0y} and ω_{0z} are the parabolic potential frequencies along the x, y and z directions, respectively. The eigenfunctions and eigenvalues of the Hamiltonian $\widehat{H}_0$ are given by

$$\psi_{n_x,n_y,n_z}(x,y,z) = \phi_{n_x}(x)\phi_{n_y}(y)\phi_{n_z}(z+\beta), \tag{2}$$

$$E_{n_x,n_y,n_z} = \left(n_x + \frac{1}{2}\right)\hbar\omega_{0x} + \left(n_y + \frac{1}{2}\right)\hbar\omega_{0y} + \left(n_z + \frac{1}{2}\right)\hbar\omega_{0z} - \frac{1}{2}\frac{e^2F^2}{m\omega_{0z}^2} \tag{3}$$

where

$$\phi_n(i) = \left(\alpha_i/\left(\sqrt{\pi}2^n n_i!\right)\right)^{1/2} exp\left(-\frac{\alpha_i i^2}{2}\right) H_{n_i}(\alpha_i i) \tag{4}$$

is the normalized wave function of the one-dimensional oscillator, $\beta = |e|F/m\omega_{0z}^2$, $\alpha_i = \sqrt{m^*\omega_{0i}/\hbar}$, $i = x, y, z$ and $H_n(x)$ is the Hermite polynomial.

2.2 Polaron states in a spherical quantum dot

The Hamiltonian of the electron-phonon interaction in a spherical quantum dot is given by [12]

$$\widehat{H}_{e-ph} = \sum_{t,\gamma}\left[V_\gamma^t(r,\theta,\varphi)a_{t\gamma} + V_\gamma^{t^*}(r,\theta,\varphi)a_{t\gamma}^+\right], \tag{5}$$

where $a_{t\gamma}\left(a_{t\gamma}^+\right)$ is the annihilation (creation) operator of the t-type phonon with frequency $\omega_{t\gamma}$ and the set of quantum numbers $\gamma = (l, m, k)$ for $t = CO$ and $\gamma = (l, m)$ for $t = SO$. The frequencies of the CO and SO optical phonons as well as electron-phonon coupling coeffcients are determined by the expressions [12]

$$\omega_{CO} = \sqrt{\frac{\epsilon_0}{\epsilon_\infty}}\omega_{TO} = \omega_{LO}, \qquad \omega_\gamma^{SO} = \sqrt{\frac{\epsilon_0 l + (l+1)\epsilon_d}{\epsilon_\infty l + (l+1)\epsilon_d}}\omega_{TO}, \tag{6}$$

$$V_\gamma^{CO}(r,\theta,\varphi) = -\sqrt{\frac{4\pi e^2\hbar\omega_{CO}}{j_{l+1}^2(\lambda_{k,l})r_0{\lambda_{k,l}}^2}}\sqrt{\frac{1}{\epsilon_\infty} - \frac{1}{\epsilon_0}}\, j_l\left(\frac{\lambda_{k,l}r}{r_0}\right)Y_{l,m}(\theta,\varphi), \tag{7}$$

$$V_\gamma^{SO}(r,\theta,\varphi) = -\frac{\sqrt{l}\epsilon_\infty\omega_{LO}}{l\epsilon_\infty + (l+1)\epsilon_d}\sqrt{\frac{2\pi e^2\hbar}{\omega_\gamma^{SO}r_0}}\sqrt{\frac{1}{\epsilon_\infty} - \frac{1}{\epsilon_0}}\left(\frac{r}{r_0}\right)^l Y_{l,m}(\theta,\varphi), \tag{8}$$

where $j_l(x)$ is the spherical Bessel function of order l, $\lambda_{k,l}$ is its k-th zero, $Y_{l,m}(\theta,\varphi)$ is the spherical harmonic function, $r_0 = \sqrt{\hbar/m^*\bar{\omega}_0}$ is the effective radius of the QD, $\bar{\omega}_0 = \sqrt[3]{\omega_{0x}\omega_{0y}\omega_{0z}}$.

The eigenfunction of the electron-phonon interaction (6) can be written as $\left|n_\gamma^t\right\rangle$, where n_γ^t shows the number of t-type phonons in the state described by the quantum number γ. We consider the electron-phonon interaction Hamiltonian (5) to be a weak perturbation of the unbeturbed

Hamiltonian (1) and derive the polaron wavefunctions and energy spectra using the first order perturbation theory. Therefore, the polaron wavefunctions and energy spectra are given by

$$|\psi_M\rangle = \left|\psi_M^{(0)}\right\rangle + \sum_{S\neq M} \frac{\left\langle\psi_S^{(0)}\right| \widehat{H}_{e-ph} \left|\psi_M^{(0)}\right\rangle}{E_M^{(0)} - E_S^{(0)}} \left|\psi_S^{(0)}\right\rangle , \tag{9}$$

$$E_M = E_M^{(0)} + \sum_{S\neq M} \frac{\left|\left\langle\psi_S^{(0)}\right| \widehat{H}_{e-ph} \left|\psi_M^{(0)}\right\rangle\right|^2}{E_M^{(0)} - E_S^{(0)}} , \tag{10}$$

where

$$\left|\psi_M^{(0)}\right\rangle = \left|\psi_{n_x,n_y,n_z}\right\rangle |n_\gamma^{SO}\rangle |n_\gamma^{CO}\rangle, \qquad M = M(n_x, n_y, n_z, \gamma) \tag{11}$$

and

$$E_M^{(0)} = E_{n_x,n_y,n_z} + \sum_\gamma \left(n_\gamma^{CO}\hbar\omega_{CO} + n_\gamma^{SO}\hbar\omega_\gamma^{SO}\right). \tag{12}$$

Further we are going to assume that the system is initially in the phonon vacuum state $|0\rangle$ and the electron-phonon interaction emits one type of phonon (SO or CO) in the mode γ. Thus (9) and (10) can be rewritten as

$$|\psi_{pol}\rangle = \left|\psi_{n_x,n_y,n_z}\right\rangle + \sum_{\substack{n\prime_x,n\prime_y,n\prime_z \\ t,\gamma}} \frac{\left\langle\psi_{n\prime_x,n\prime_y,n\prime_z}\right| \widehat{H}_{e-ph} \left|\psi_{n_x,n_y,n_z}\right\rangle}{E_{n_x,n_y,n_z} - E_{n\prime_x,n\prime_y,n\prime_z} - \hbar\omega_\gamma^t} \left|\psi_{n\prime_x,n\prime_y,n\prime_z}\right\rangle , \tag{13}$$

$$E_{pol}^{(M)} = E_{n_x,n_y,n_z} + \sum_{\substack{n\prime_x,n\prime_y,n\prime_z \\ t,\gamma}} \frac{\left|\left\langle\psi_{n\prime_x,n\prime_y,n\prime_z}\right| \widehat{H}_{e-ph} \left|\psi_{n_x,n_y,n_z}\right\rangle\right|^2}{E_{n_x,n_y,n_z} - E_{n\prime_x,n\prime_y,n\prime_z} - \hbar\omega_\gamma^t} , \tag{14}$$

2.3 Differential cross-section for polaronic Raman scattering

The general expression for the Raman scattering differential cross-section is given by [13]

$$\frac{d^2\sigma}{d\omega_s d\boldsymbol{\Omega}} = \frac{V^2\omega_s^2 n(\omega_s)}{8\pi^3 c^4 n(\omega_i)} W(\hbar\omega_i, \boldsymbol{e}_i; \hbar\omega_s, \boldsymbol{e}_s), \tag{15}$$

where c is the speed of light, $n(\omega)$ is the refraction index as a function of the radiation frequency, $\boldsymbol{e}_s$ and $\hbar\omega_s$ ($\boldsymbol{e}_i$ *and* $\hbar\omega_i$) are the polarization vector and photon energy of the emitted secondary (absorbed incident) radiation field respectively, $V = 4\pi^2 r_0^3/3$ is the QD volume. The transition probability $W(\hbar\omega_i, \boldsymbol{e}_i; \hbar\omega_s, \boldsymbol{e}_s)$ is given by [13]

$$W(\hbar\omega_i, \boldsymbol{e}_i; \hbar\omega_s, \boldsymbol{e}_s) = \frac{2\pi}{\hbar} \sum_f |M(\hbar\omega_i, \boldsymbol{e}_i; \hbar\omega_s, \boldsymbol{e}_s)|^2 \delta\left(E_f - E_i\right) \tag{16}$$

where

$$M(\hbar\omega_i, \boldsymbol{e}_i; \hbar\omega_s, \boldsymbol{e}_s) = \sum_p \frac{\left\langle f\left|H_{rad}^{(s)}\right|p\right\rangle\left\langle p\left|H_{rad}^{(i)}\right|i\right\rangle}{E_i - E_p + i\,\Gamma_p/2} + \sum_q \frac{\left\langle f\left|H_{rad}^{(i)}\right|q\right\rangle\left\langle q\left|H_{rad}^{(s)}\right|i\right\rangle}{E_i - E_q + i\,\Gamma_q/2} \tag{17}$$

Here $|i\rangle$ and $|f\rangle$ denote the initial and final states of the system corresponding to energies E_i and E_f, $|p\rangle(|q\rangle)$ is the intermediate state corresponding to the energy $E_p(E_q)$, $\Gamma_p(\Gamma_q)$ is a lifetime broadening parameter. The initial state $|i\rangle$ consists of a polaron with energy $E_{pol}^{(i)}$ and an incident photon of energy $\hbar\omega_i$ ($E_i = E_{pol}^{(i)} + \hbar\omega_i$). The intermediate state $|t\rangle(t = p, q)$ includes a polaron in an excited state with energy $E_{pol}^{(t)}$ ($E_t = E_{pol}^{(t)}$) . The final state $|f\rangle$ contains a polaron in an excited state and a scattering photon of energy $\hbar\omega_s$ ($E_f = E_{pol}^{(f)} + \hbar\omega_s$). Therefore $E_i - E_t = E_{pol}^{(i)} + \hbar\omega_i - E_{pol}^{(t)} = E_{pol}^{(f)} + \hbar\omega_s - E_{pol}^{(t)}$. In Eq. (16) we have approximated the Dirac delta function as follows:

$$\delta(E_f - E_i) = \frac{1}{\pi} \frac{\Gamma_f}{(E_f - E_i)^2 + \Gamma_f^2} \tag{18}$$

The operator $H_{rad}^{(i)}(H_{rad}^{(s)})$ describes the interaction with the incident(emitted) radiation field in the dipole approximation

$$H_{rad}^{(i)} = \frac{|e|}{m_0}\left(\frac{2\pi\hbar}{V\omega_i}\right)^{1/2} \boldsymbol{e}_i \cdot \hat{\boldsymbol{p}}, \qquad H_{rad}^{(s)} = \frac{|e|}{m^*}\left(\frac{2\pi\hbar}{V\omega_i}\right)^{1/2} \boldsymbol{e}_s \cdot \hat{\boldsymbol{p}}, \qquad \hat{\boldsymbol{p}} = -i\hbar\boldsymbol{\nabla}, \tag{19}$$

where m_0 is the bare electron mass. In (18) we have neglect the difference between electron and polaron effective masses.

3. Numerical results and discussion

In this section, the Raman scattering differential cross-section of a CdSe spherical QD in the presence of a uniform electric field as a function of $\hbar\omega_s$ is investigated numerically. The values of physical parameters are chosen as: $m^* = 0.13m_0$, $\epsilon_0 = 9.56$, $\epsilon_\infty = 6.23$, $\epsilon_d = 1$, $\hbar\omega_{LO} = 26.46$ meV and $\hbar\omega_{TO} = 21.36$ meV [14]. We have set $\Gamma_p = \Gamma_q = 3$ meV, $\Gamma_f = 1$ meV. We consider that the polarization vectors of incident and scattered radiations are along the y-axis. Because the resonant peaks corresponding to different transitions can appear at the same photon energies we only present a few transitions with unique peak positions at all spectra. In all the plots the peak positions mediated by photons do not depend on the incident radiation energy and only depend on the difference of the subbands involved in the transition.

Fig. 1 is the numerical representation of the electron (solid lines) and polaron (dotted lines) energies for differend states as a function of the dot radius. Naturally, the energy of the electron in different states decreases as the radius of the quantum dot increases, since the spatial confinement of particle motion weakens. At the same time, it should be noted, that the difference between the energies of the polaron and electron states with the same quantum numbers decreases with increasing quantum numbers. This pattern is also clearly visible in Table 1, in which the energy values of the electron and polaron for states (0,0,0), (0,0,1), (0,1,1), (1,1,1), (1,1,2) and (1,2,2) are presented at quantum dot radii $2nm$, $2.5nm$ and $3\ nm$.

In Fig. 2 the emission spectrum for parallel polarizations of the incident and secondary photon is shown forQD radii $r_0 = 2\,nm$, $r_0 = 2.5\,nm$ and $r_0 = 3\,nm$ and electric field strength $F = 1\,kV/cm$. The excitation energy is $900\,meV$. Here we can observe the appearance of peaks due to photon emission. The solid (red) lines and blue (dotted) lines correspond to electron and polaron transitions, respectively. It should be noted that, due to the strong spatial confinement of the electron (polaron), the effect of the electric field on the states is insignificant.

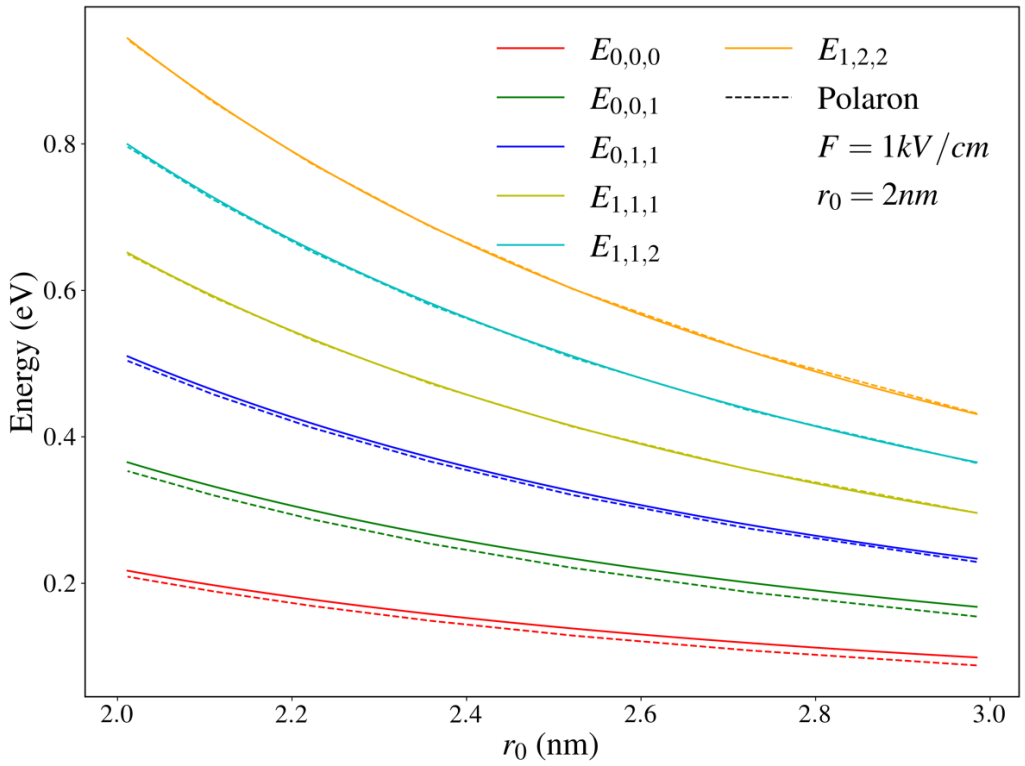

Fig. 1. Electron and a polaron energies in different quantum states depending on the radius of the quantum dot at electric field strength F= 1kV/cm.

Table 1. Electron and polaron energies for the states (0,0,0), (0,0,1), (0, 1,1), (1, 1,1), (1, 1,2) and (1, 2,2) at quantum dot radii 2nm, 2.5nm and 3 nm

	Quantum states (n_x, n_y, n_z)					
	0,0,0	0,0,1	0,1,1	1,1,1	1,1,2	1,2,2
Dot radius (r_0)	Polaron energies (in meV)					
$2nm$	208.95	353.09	503.67	649.17	795.87	942.24
$2.5nm$	130.51	224.18	324.87	419.52	514.88	610.11
$3nm$	84.51	150.58	222.11	286.19	351.7	417.48
Dot radius (r_0)	Electron energies (in meV)					
$2nm$	217.11	365.14	509.89	651.34	799.38	944.12
$2.5nm$	140.13	236.85	330.27	420.41	517.13	610.55
$3nm$	95.39	164.48	226.98	286.19	355.28	417.78

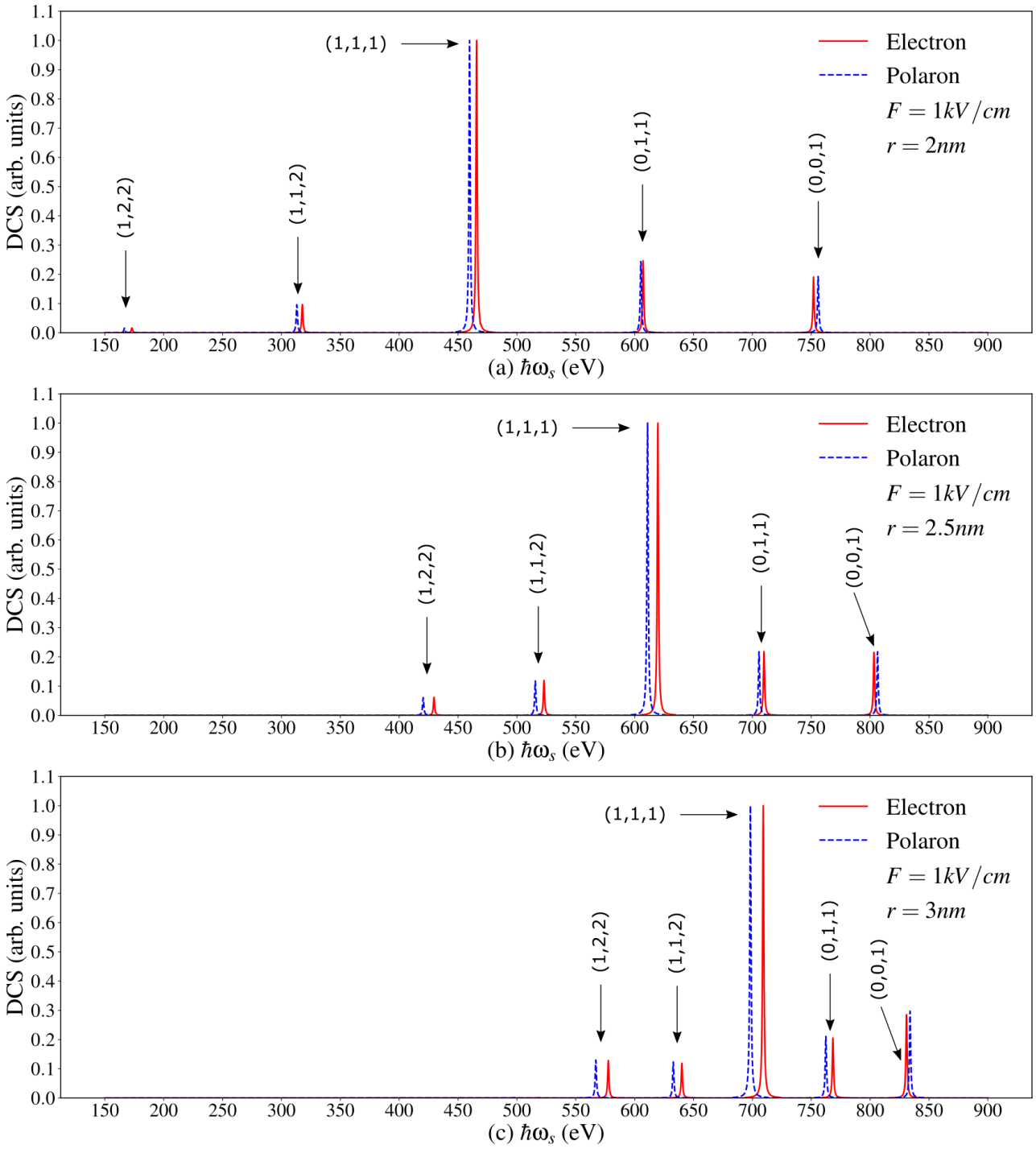

Fig. 2. DCS as a function of emitted photon energy $\hbar\omega_s$ for transitions from a few excited states to the ground state ($E_{0,0,0}$) in case of $\hbar\omega_i = 900\ meV$, $F = 1\ kV/cm$ for wire radii (a) $r_0 = 2\ nm$, (b) $r_0 = 2.5\ nm$, (c) $r_0 = 3\ nm$.

4. Conclusions

In summary, we have presented a formal method for the calculation of the Raman differential cross-section for polaron Raman scattering in a semiconductor quantum dot, considering a homogeneous electric field. The main feature of polaron Raman scattering is the appearance of a rich multi-frequency spectrum, due to the non-equidistance of polaron energy levels, as wel as the presence of a selection rule for transitions with a change in quantum numbers n_x, n_y, n_z. The theoretical study of the dependence of the differential cross section on the frequency parameters of

the system, which determine the energy spectrum of an electron, can be used for the spectroscopic characterization of such systems.

Acknowledgments

The work was supported by the Science Committee of RA, in the frame of the research projects No. 21AG-1C048, No. 20TTWS- 1C014 and No. 21AA-1C021.

References

[1] A. Tartakovskii, Quantum Dots: Optics, Electron Transport and Future Applications (Cambridge University Press, Cambridge, 2012).
[2] T.D. Krauss, F.W. Wise, Phys. Rev. B **55** (1997) 9860.
[3] A.G. Milekhin, D.A. Tenne, D.R.T. Zahn, Quantum Dots and Nanowires, (Am. Sci., Stevenson Ranch, California, 2003).
[4] T. Livneh, J. Zhang, G. Cheng, M. Moskovits, Phys. Rev. B **74** (2006) 035320.
[5] J. Wang, F. Demangeot, R. Pechou, A. Ponchet, A. Cros, B. Daudin, Phys. Rev. B **85** (2012) 155432.
[6] V. Laneuville, F. Demangeot, R. Péchou, P. Salles, A. Ponchet, G. Jacopin, L. Rigutti, A. de Luna Bugallo, M. Tchernycheva, and F. H. Julien, K. March and L. F. Zagonel R. Songmuang, Phys. Rev. B 2011, **83**, 115417.
[7] N.B. Margaryan, N.E. Kokanyan, E.P. Kokanyan, J. Contemp. Phys. **56** (2021) 260.
[8] X. Guo, C. Liu, Chin. J. Phys. **56 (2018)** 1894.
[9] A. Tiutiunnyk et al., V. Akimov, V. Tulupenko, M.E. Mora-Ramos, E. Kasapoglu, A.L. Morales, C.A.Duque, Eur. Phys. J. B **89** (2016) 107.
[10] M.J. Karimi, G. Rezaei, H. Pakarzadeh, Phys. Lett. A **377** (2013) 2164.
[11] W. Xie, Chem, Phys. **423** (2013) 30.
[12] J.C. Marini, B. Stebe, E. Kartheuser, Phys. Rev. B **50** (1994) 14302.
[13] R. Betancourt-Riera, J.M. Bergues, R. Riera, J.L. Marin, Physica E **5** (2000) 204.
[14] A. Vartanian, L. Vardanyan, Superlattice. Microst. **119** (2018) 224.